

Assessment of Fermi-liquid description for the normal state of high- T_c superconductors

Ju H. Kim and K. Levin

Department of Physics, The University of Chicago, James Franck Institute, Chicago, Illinois 60637

A. Auerbach*

Physics Department, Brookhaven National Laboratory, Upton, New York 11973

(Received 25 July 1988; revised manuscript received 26 October 1988)

The applicability of Fermi-liquid theory for the normal state of the high- T_c copper oxides is investigated. In the present context "Fermi-liquid theory" refers to a description in which there are two components (copper and oxygen) within the Fermi surface. This is to be contrasted with other approaches in which the Cu electrons are fully localized. Our calculations are based on a Coulomb renormalized band structure which characterizes the quasiparticle energies. This band structure arises from a variety of different but essentially equivalent mean-field techniques. The present focus is on deriving a Fermi-liquid description which combines both Coulomb-induced localization (as a precursor to the insulating state) with semirealistic band structure. The latter requires that next-nearest-neighbor oxygen-oxygen overlap integrals also be included in a tight-binding scheme. The interplay of these two effects leads to (i) a positive Hall coefficient which becomes progressively larger as the insulator is approached and reverses its sign for large doping concentration; (ii) a "pinning" of the Cu valence near the Cu^{2+} state; (iii) two important features in the density of states, one of which can be associated with the van Hove singularities and the other with band narrowing or incipient localization effects. The former occur away from the half-filled limit as a result of oxygen-oxygen overlap processes, so that the perfect nesting of the nearest-neighbor half-filled tight-binding model is significantly offset. The latter leads to a strong prediction of the theory: as in the Brinkman-Rice picture, incipient localization effects will be manifested by a progressively larger Sommerfeld coefficient γ as the insulator is approached. This prediction needs to be tested experimentally. While transport experiments seem consistent with this behavior, more direct thermodynamic measurements are both difficult to interpret and too sample sensitive to allow clear trends to be inferred from the data. Our general conclusion is that, at present, there is no persuasive evidence to support the claim that Fermi-liquid theory is inapplicable to the copper oxides.

I. INTRODUCTION

One of the key questions in the newly discovered high- T_c copper-oxide materials is whether the normal state is properly described by Fermi-liquid theory. In a strict sense a Fermi-liquid description is only meaningful at $T=0$. Here we use the term loosely to characterize the state above T_c which evolves continuously from the low-temperature Fermi liquid. While it is clear that a full understanding of the normal state may not unambiguously reveal the superconducting mechanism, it is unlikely that the latter can be understood without a detailed theoretical picture of normal-state properties. It is the purpose of this paper to consider a number of important issues which will help to assess the validity of Fermi-liquid theory. We focus on two criteria which we argue must be obeyed in order to build a satisfactory picture of the Fermi liquid (if indeed it does exist): the Fermi liquid must break down slightly below the half-filled limit as a result of a (localization-driven^{1,2}) metal-insulator transition and it must yield a holelike character of the Fermi surface or quasiparticles as seems to be unambiguously observed in Hall coefficient measurements. While there are other ingredients (e.g., magnetic effects) which may ultimately be incorporated into a complete theory it is our opinion that these two criteria are essential in describing the "quasi"

particles or renormalized band structure in the Fermi liquid.

There are two rather distinct theoretical approaches to the normal-state properties: those which are based on a Fermi-liquid picture³⁻⁸ and those^{9,10} whose starting point is the half-filled limit where an insulating Heisenberg antiferromagnet is observed.¹¹ In strict Fermi-liquid approaches, Luttinger's theorem¹² is manifestly obeyed so that the Fermi surface volume is invariant under interaction effects. As in the noninteracting system, both the copper and oxygen electrons are included in this volume. In theories based on a two-component magnetic insulator,⁹ the copper oxides correspond to a disordered Heisenberg antiferromagnet composed of Cu spins in the presence of dilute, mobile oxygen holes. In this way the copper electrons are assumed to be *fully* localized even in the metallic regime and Luttinger's theorem is not obeyed. Split-band descriptions of the Hubbard type are often used as a basis for these oxygen hole "Fermi liquids." However, the absence of a sharp Fermi surface in the Hubbard alloy analogy scheme may make a Fermi-liquid picture, even in this looser interpretation, problematic. Here we will use the term "Fermi liquid" only in the conventional sense so that it applies to those systems in which Luttinger's theorem is satisfied.

Experiments are not presently capable of definitively

determining the validity of a Fermi-liquid approach. Positron annihilation experiments¹³ in $\text{YBa}_2\text{Cu}_3\text{O}_7$ are interpreted as yielding evidence for a Fermi surface, which has several features in common with that obtained from band-structure calculations and seems to satisfy Luttinger's theorem. Korringa-type behavior of Cu NMR relaxation¹⁴ in doped La_2CuO_4 may also support the existence of a Fermi liquid in the normal state, as may recent photoemission data.^{14(a)} However, the two "canonical" Fermi-liquid properties, the Pauli susceptibility and linear (in temperature) coefficient of the specific heat, have not yet been unambiguously measured. The latter is difficult to observe above the relatively high transition temperatures of the superconducting phase.¹⁵ For the former there seems to be conflicting interpretations. In both La_2CuO_4 doped with Sr, and $\text{YBa}_2\text{Cu}_3\text{O}_7$, χ is extremely sensitive to the oxygen content.¹⁶⁻²⁰ Furthermore, only in a narrow region of oxygen and/or strontium concentration (corresponding to the highest- T_c superconductors in each family) does the measured χ exhibit temperature-independent behavior.¹⁶⁻²⁰ The observed temperature dependence has been attributed¹⁷ to isolated magnetic defects and impurities and is compensated for by Curie-Weiss subtractions. In $\text{YBa}_2\text{Cu}_3\text{O}_7$ sample dependences¹⁹ seen in single crystals are attributed to minute variations in oxygen content. Furthermore, varying degrees of oxygen ordering in the chains²⁰ are believed to lead to different dependences on the oxygen concentration in the Pauli susceptibility. Until better samples with controlled stoichiometries are made, it will not be possible to obtain direct measurements of the Pauli susceptibility and linear specific-heat coefficient (if indeed these contributions are present).

Among the most persuasive arguments in favor of a Fermi-liquid description for the copper oxides is the unambiguous observation of Fermi-liquid behavior in the closely related and very strongly correlated heavy-fermion metals.^{21,22} The copper oxides are often described by the same (Anderson lattice) Hamiltonian²³ as the heavy-fermion materials.²⁴ This Hamiltonian contains a hybridization between local Cu d levels with neighboring oxygen electrons and strong on-site Coulomb correlations between the Cu states. Despite the similar starting point for the heavy fermions and copper oxides there are important differences. In the heavy fermions, the conduction band contributes a metallic conductivity even when the f band is near the half-filled limit. In the copper oxides, the oxygen band becomes full when the d band is half full, so that these systems are insulators.

There has been considerable theoretical progress in the solution of the Anderson lattice Hamiltonian and its relationship to Fermi-liquid theory in the context of heavy fermion systems.²⁴⁻²⁸ Most important, a number of different theoretical approaches have arrived at a similar picture of the Fermi-liquid state in which the "quasiparticles" are described by a Coulomb renormalized band structure.²⁴⁻²⁸ In addition to the similarities with the heavy fermions, it is widely believed that the proximity to a metal-insulator transition is an important aspect of the high-temperature superconductors.²⁹ Indeed, one can hope to gain insight into this transition by studying its counterpart in other

transition-metal oxides.³⁰⁻³⁵ One-band Hubbard models have been addressed using both the Hubbard alloy analogy³³ which violates Luttinger's theorem as well as a Gutzwiller trial wave-function³⁴ approach which does not properly describe the ground state of the insulating antiferromagnet.³⁵ However, because of the moderate success of the Gutzwiller (Brinkman-Riu) picture in understanding the metal-insulator transition as approached from a Fermi-liquid state, one would like to study it (or other similar mean-field schemes such as the $1/N$ expansion approach) in the two-band copper-oxide model. We are, thus, led by analogies to both the heavy fermions and transition-metal oxides to apply to the Anderson lattice Hamiltonian these mean-field theoretic techniques.

How much is known about the nature of the metal-insulator transition in the copper-oxide materials? It is unlikely that this transition is driven by the opening of an antiferromagnetic gap due to Fermi-surface nesting since (i) the materials are insulating even when the long-range antiferromagnetic order has disappeared¹¹ as a result of doping. (ii) If the insulator were driven by a spin-density-wave gap then it would not appear precisely at the half-filled point. Direct calculations of the wave-vector-dependent susceptibility for a realistic band structure³⁶ show that the optimal (hole) concentration for nesting may be significantly offset from the half-filled point. It is more reasonable to expect that the insulating transition derives from Coulomb-induced localization of the Cu electrons, as has been observed in other transition-metal oxides.³⁴ This would lend support to Heisenberg-type models of the pure material, La_2CuO_4 , which seem to correctly describe the spin dynamics^{37,38} observed in neutron scattering¹¹ experiments.

Newns and his collaborators⁷ as well as Kotliar, Lee, and Read⁶ have studied the mean-field solutions to the Anderson lattice Hamiltonian based on the $1/N$ expansion technique (with infinite Coulomb correlations) in the context of the copper oxides. This body of work is in the same spirit as that of the present paper. We stress that the conclusions of these previous and the present calculations are not peculiar to the $1/N$ scheme but are more generally valid for a class of mean-field theories.²⁴⁻²⁸ In Refs. 6 and 7, the focus is on a "hole picture." This hole picture is associated with an infinite Coulomb repulsion between holes so that the valence state Cu^{3+} is never present. In an "electron picture" (for less than half filling), an infinite electron-electron repulsion requires that the valence state Cu^{1+} is never observed. The terms electron or hole picture pertain only to the valence states present and not to the sign of the charge carriers, such as would be measured in a Hall experiment.

In the present work, we will argue that the d electron Coulomb repulsion U_d is not so large as to completely exclude a third (minority) valence state. However, while we cannot yet treat this finite U_d limit, we assume that the *essential* role of Coulomb correlations is to lead to the breakdown of the Fermi-liquid sufficiently close to the half-filled point. The character of the various copper valence states which are present is of lesser importance. We have found that in order to obtain this metal-insulator transition within the hole picture, the ratio of the copper-

oxygen hybridization to the hole level splitting must be less than 0.2. Thus, the transition was found in Ref. 6 but not in Ref. 7, where a more realistic tight-binding fit to the band structure was incorporated. To simulate the effects of the localization transition on the Fermi liquid we may work either in the hole picture, provided we assume a somewhat unphysical, highly ionic limit, or in the electron picture where the band structure may be treated more realistically. We have chosen the latter alternative, since we wish to focus on a more plausible band structure and its relationship to the localization transition.

There has been much discussion in the literature concerning the valence state of Cu in the metallic copper oxides.^{4,5,39-45} Theoretical approaches,^{23,40} for the most part, indicate that the valence states are Cu^{1+} and Cu^{2+} . Spectroscopic measurements suggest that copper is primarily in the Cu^{2+} state even in materials which contain excess holes. It should be noted that because of the nature of oxygen-deficient surfaces in ultrahigh vacuum and uncertainties in the Cu valence of the reference materials, the various spectroscopies do not yet yield definitive results.⁴¹ Furthermore, there are conflicting experimental interpretations; some investigators purport to see^{4,5} only Cu^{2+} ; others report the two valence states:⁴² Cu^{2+} , Cu^{3+} , while some groups claim^{40,43} that only Cu^{2+} and Cu^{1+} are present. Furthermore, there are claims that the valence state is strongly affected by oxygen stoichiometry.⁴⁴ Finally, some groups argue that all three valence states⁴⁵ are present in the same sample, although this appears to be a consequence of the two distinct (chain/plane) copper sites in $\text{YBa}_2\text{Cu}_3\text{O}_7$. In the localization model discussed here, Cu^{2+} is by far the dominant valence state. However, in any system with excess holes, there will be a small but finite concentration of Cu^{3+} reflecting the fact that in a covalent system, the holes are shared (albeit unequally) among oxygen and copper. This Cu^{3+} should not be viewed, then, as an ionic state of copper, but rather as a hybridized $3d^9L$ state.

In order to clarify the various pictures discussed above it is instructive to plot schematically the behavior of the Coulomb renormalized band structure in the uppermost bands as the electron filling is increased about the half-filled point. This is shown in Fig. 1 for three different models where the labels (a)–(d) refer to (a) less than half filled, (b) slightly less than half filled, (c) slightly more than half filled, and (d) more than half-filled bands. The Cu^{1+} and Cu^{2+} mixed valence model of Ref. 7 is shown in the left-most sequence of figures. In the middle sequence the results of the localization driven metal-insulator transition are shown for the same values of electron filling. Finally, in the right-hand panel are shown the results of the Hubbard alloy analogy³³ in which there is a splitting of the (single) band which results from the particular way in which the Coulomb correlations are treated.

In the hole picture, (left most panel) the antibonding band is narrowest at considerably less than half filling. This is because an increasing concentration of holes is associated with a decreasing amount of Cu^{1+} , and hence less mixed valency. As more electrons are added it then widens progressively without showing any distinctive behavior at the half-filled point. By contrast in the localiza-

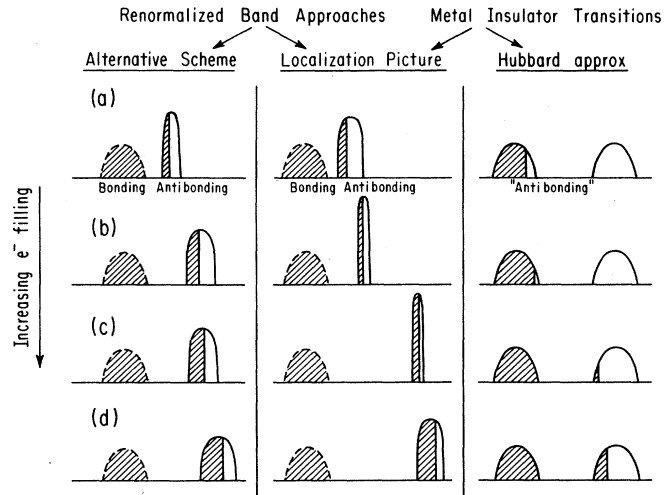


FIG. 1. Schematic representation of band structure as it evolves under variations in the electron filling near the half-filled limit. Left-most panel corresponds to the renormalized band approaches of Ref. 7, central panel represents the localization picture of the present paper and Ref. 6, and panel at right corresponds to Hubbard alloy analogy scheme. Labels (a) and (d) refer to below and above half filling, respectively; labels (b) and (c) refer to very slightly below and very slightly above the half-filled point.

tion picture, the antibonding band approaches a δ function at half filling from both directions. However, depending on the direction of approach this δ function is shifted in energy (in the “electron picture”) by roughly the magnitude of the Coulomb interaction. This is the only manifestation of the Coulomb “gap” effect seen in the Hubbard approximation. In this latter approximation (right panel) the half-filled point also corresponds to an insulating state, which arises, as in a semiconductor from a band splitting effect. It has been argued³⁹ that a natural extension of the Sawatzky-Allen³¹ picture to the doped copper oxides would lead to a picture similar to that shown by the Hubbard approximation of Fig. 1, but with the lower band corresponding to the oxygen $2p$ and the upper band to the copper $3d$ electrons. The band gap is, thus, of the “charge transfer” variety. Furthermore there would be a third band (whose counterpart is not shown in the right-hand panels of the figure) which is a filled copper $3d$ band containing one copper electron.

In physical terms, the distinction between the localization and Hubbard pictures of the metal-insulator transition is that in the former the effective mass m^* approaches infinity, whereas in the latter the carrier density n approaches zero at the insulating limit. From this point of view the Hubbard picture is analogous to other non-Fermi-liquid models^{9,10} in which the carrier density n approaches 0 at half filling. For optical properties, for example, which depend on the ratio n/m^* , there will be no apparent difference between the two pictures. Kotliar, Lee, and Read⁶ were able to explain low-frequency conductivity data by assuming a large effective mass (which approaches infinity at the half-filled point). Alternatively

these data have been interpreted to suggest a small carrier concentration which vanishes at the insulating limit. However, we might expect that other properties such as the Hall coefficient would help distinguish between the two descriptions. It is therefore not surprising that Hall measurements have been viewed as a key test of Fermi-liquid theory in the copper oxides. To address these issues, much of the present paper will be devoted to a discussion of the Hall coefficient R_H .

Hall experiments are also important in helping to ascertain the correct "sign" of the charge carriers. In a Fermi-liquid scheme, this sign is a measure of the *shape* of the Fermi surface as distinguished from its *volume*. Using a Boltzmann equation approach⁴⁶ to calculate R_H , we shall show here that in the simplest nearest-neighbor tight-binding model of the copper oxides, the Hall coefficient has the wrong (negative) sign. Furthermore, because of the perfect nesting of the Fermi surface, the Hall coefficient vanishes identically at the half-filled point. These results which are consequences of the "bare" or nonrenormalized band structure are not altered by the inclusion of (infinitely strong) Coulomb correlations. To obtain a positive Hall coefficient, as is observed experimentally⁴⁷⁻⁵⁰ in all families of the high- T_c superconductors, it is necessary to modify this bare band structure to include direct in-plane oxygen-oxygen overlap or hybridization processes. These next-nearest-neighbor processes coupled to the planar copper-oxygen hybridization terms simulate remarkably well the dominant features of the Fermi-surface shape found in more complete band-structure approaches,³⁶ for a range of hole concentrations.

Experimentally, it is observed that as the materials approach the insulating limit, the *magnitude* of the Hall coefficient grows rapidly, much more so than is consistent with band-structure calculations. The data suggest that R_H varies as $1/x$ where x is the hole concentration (or Sr concentration per Cu atom in La_2CuO_4). It has been claimed that such behavior is inconsistent with Fermi-liquid theory. A naive argument (based on a parabolic free-electron band) would yield a Hall coefficient varying as $1/(1+x)$, since the Cu atoms also contribute one hole. On this basis it has been argued⁴⁷ that a non-Fermi-liquid theory might be more appropriate. However, we will show here that the strong x dependence of R_H is also compatible with a Coulomb renormalized band-structure (which is nonparabolic) and that it arises in a theory such as ours, from incipient localization of the Cu d electrons near the half-filled limit.

We do not address the temperature dependence of the resistivity which has also been interpreted as signaling the breakdown of Fermi-liquid theory. This will be a topic of a future paper. Recently a Fermi-liquid-based explanation of the linear temperature dependence has been suggested.^{46,51} This linear dependence has been attributed to an electron-phonon scattering mechanism. However, simple band-structure approaches⁴⁶ are not able to explain the large magnitude of this contribution and it is argued that the Fermi velocity may be overestimated. In a similar way the authors of Ref. 51 are led to the conclusion that there exists some band-narrowing effect which must be invoked to understand the large size of the linear term.

We note that these conclusions are suggestive of a large mass enhancement (which does not derive from electron phonon coupling) such as would be found in the present theory. Additionally, because the slope (with respect to temperature) of the resistivity has been observed¹⁸ to increase as the insulator is approached, this may be interpreted as further evidence for an increase in the transport mass near the insulating limit.

We conclude with a note of caution. Our results indicate that Fermi-liquid theory may not be inapplicable. This does not imply that a Fermi-liquid approach is necessarily correct. Non-Fermi-liquid schemes have also successfully explained¹⁰ transport data.

II. FORMAL RESULTS

A. Mean-field approach to copper-oxide Hamiltonian

The Anderson lattice Hamiltonian is a useful starting point for treating the copper-oxide planes in the various high T_c , copper-oxide-based materials. There are two neglected contributions in this Hamiltonian: The Coulomb repulsion on the oxygen sites and the intersite Coulomb term. Recent work by McMahan, Martin, and Satpathy²³ suggests that omitting these two terms may be reasonable approximations. Using density-functional schemes, these authors claim that the intersite Coulomb repulsion is relatively small. While the Coulomb interactions on the oxygen sites are not insignificant, because the intrinsic bandwidths associated with the oxygen atoms are rather large, this reduces the effectiveness of the oxygen Coulomb repulsion. The CuO_2 model on a lattice is written as

$$H = \sum_{j,\sigma} \varepsilon_p C_{j,\sigma}^\dagger C_{j,\sigma} + \sum_{i,\sigma} \varepsilon_d^0 D_{i,\sigma}^\dagger D_{i,\sigma} + \sum_{i,j,\sigma} V_{i,j} (C_{j,\sigma}^\dagger D_{i,\sigma} + D_{i,\sigma}^\dagger C_{j,\sigma}) + \sum_i U_d n_{i,\uparrow} n_{i,\downarrow}, \quad (2.1)$$

where ε_p and ε_d^0 are the oxygen and (unrenormalized) copper energy levels, $C_{j,\sigma}^\dagger (C_{j,\sigma})$ and $D_{i,\sigma}^\dagger (D_{i,\sigma})$ are creation (destruction) operators for oxygen electrons at site j and spin σ and copper electrons at site i , with spin σ , respectively. $V_{i,j}$ is a hopping integral between nearest copper and oxygen sites, and $n_{i,\sigma} = D_{i,\sigma}^\dagger D_{i,\sigma}$. The Coulomb repulsion between electrons on Cu sites is U_d .

Within the copper oxides, there are presumably three valence states of copper which may be present: Cu^{2+} , Cu^{3+} , and Cu^{1+} corresponding, respectively, to the $3d^9$, $3d^8$, and $3d^{10}$ atomic configurations. We, therefore, begin with a reformulation of the CuO_2 Hamiltonian which includes all three valence states. As originally proposed by Newns and co-workers,⁷ the Hamiltonian may be rewritten using an enlarged Hilbert space of bosons and fermions. This auxiliary boson technique was first introduced by Barnes⁵² for the Kondo impurity problem and has since proved useful for the heavy fermions as well. We will treat both the electron and hole pictures separately. This distinction is made so that we can ultimately approximate the Hamiltonian by the $U_d \rightarrow \infty$ limit. This requires that U_d be larger than any other energy scale in the

problem. Which of the two pictures is more appropriate depends on the relative size of the Coulomb repulsion as compared with the electron or hole level splitting. When U_d is large compared to $|\varepsilon_d^0 - \varepsilon_p|$ we are in the electron picture, whereas when U_d is large compared to $|\varepsilon_p - (\varepsilon_d^0 + U_d)|$ we are in the hole picture. We begin with the electron picture. In the limit of infinite U_d only two valence states will be present. For less than half filling of the uppermost band, the allowed valence states are Cu^{2+} and Cu^{3+} . For more than half filling the two mixed valence states are Cu^{2+} and Cu^{1+} . In each case the second valence state is represented by a boson field which is treated in the usual mean-field approximation.²⁵⁻²⁸ Clearly, for infinite Coulomb interactions, only one of the two boson fields is present. In this mean-field approach, it is convenient to introduce a local gauge transformation which avoids an unphysical gauge symmetry breaking. Variational^{27,28} as well as $1/N$ expansion techniques^{25,26,53,54} all reduce to essentially equivalent mean-field results. Here N is the spin degeneracy of the copper and oxygen spin states. A Lagrange multiplier λ_0 is introduced to impose the constraint associated with infinite Coulomb interactions. The resulting mean-field Hamiltonian may be readily diagonalized to yield a renormalized band structure

$$E^\pm(k) = \frac{\varepsilon_p + \varepsilon_d}{2} \pm \left[\left(\frac{\varepsilon_p - \varepsilon_d}{2} \right)^2 + e_0^2 \gamma_k^2 \right]^{1/2}, \quad (2.2)$$

where

$$\gamma_k = 2V \left[\cos^2 \left(\frac{k_x a}{2} \right) + \cos^2 \left(\frac{k_y a}{2} \right) \right]^{1/2},$$

and $\varepsilon_d = \varepsilon_d^0 + \lambda_0$ is a renormalized copper energy level. Here e_0 is the mean value of the boson field. Self-consistent equations for the unknown band parameters e_0 and λ_0 are obtained variationally. It should be noted that in this mean-field approach when the d band is more than half full, it is relatively easy to violate particle number conservation which may, incorrectly, be viewed as leading to superconductivity. In our calculations care is taken to avoid these problems and to insure that the number operator commutes with the mean-field Hamiltonian. To illustrate this point further, one can consider a mean-field theory in which both the Cu^{3+} and the Cu^{1+} bosons are simultaneously nonzero as would be appropriate at finite U_d . In this case it is not possible to introduce a mean-field theory which avoids a broken gauge symmetry. There is clearly a qualitative difference between the single boson and double boson mean-field theories and it is not surprising that the latter necessarily leads to "superconductivity."⁷

Several authors have used the auxiliary boson technique in the CuO_2 Hamiltonian, but within a hole rather than particle picture.^{6,7} In this picture, the hole energies are related to their electronic counterparts as

$$\tilde{\varepsilon}_p = -\varepsilon_p, \quad \tilde{\varepsilon}_d^0 = -(\varepsilon_d^0 + U_d), \quad \tilde{V}_{i,j} = -V_{i,j}. \quad (2.3)$$

In order to have a sensible theory, the bare hole energy $\tilde{\varepsilon}_d^0$ is assumed to be finite, although in the Coulomb (hole) repulsion term U_d is taken to be infinite. A mean-field approximation combined with a local gauge transformation

is introduced, as in the particle picture discussed above. Because the particle and hole Hamiltonians are readily interrelated, the self-consistent equations as well as renormalized band structures can be easily obtained from their counterparts in the particle picture. It should be stressed that because of the inequivalent ways in which the Coulomb repulsion is treated in the electron and hole pictures (i.e., U_d is taken to be finite in the single-particle energy and infinite elsewhere), the resulting physics is different in the two pictures even when the valence assignments are assumed to be same.

It is useful at this point to review the relatively simple physics which arises from the mean-field approximation. The effects of infinite Coulomb correlations are twofold: the hybridization is renormalized as follows

$$V_{i,j} \rightarrow V_{i,j} e_0, \quad (2.4)$$

and the d level

$$\varepsilon_d^0 \rightarrow \varepsilon_d^0 + \lambda_0. \quad (2.5)$$

These two renormalizations are needed to avoid multiple occupancy of the d level. The hybridization reduction factor is given by the bose amplitude e_0 where $e_0^2 = 1 - n_d$ and $n_d \leq 1$ is the number of d electrons at each copper site. Furthermore, the d level is raised to a position near the Fermi energy in order to accommodate not more than one d electron per site. The system approaches the insulating state as $e_0 \rightarrow 0$ and $n_d \rightarrow 1$ and at the same time the effective mass becomes infinite (as in the Gutzwiller picture³⁴). At this point there are no Cu^{3+} states and the system has only a localized Cu^{2+} at each site. This coincides with the filling of the oxygen bands. For the models we will consider here, the system is insulating when the total number of electrons is five, corresponding to four oxygen electrons (in the two p_x, p_y bands) and one copper electron. It follows from Eq. (2.4) that as e_0 decreases, the conduction band narrows as shown schematically in Fig. 1 (central panel).

Similarly, an insulating state will also be reached when approached from above (i.e., $n^{\text{tot}} > 5$). At the half-filled point $n^{\text{tot}} \rightarrow 5$ the system will choose not to put any electrons in the Cu^{1+} state, because of the large Coulomb repulsion. In this way at half filling only localized Cu^{2+} will be present. There is clearly a discontinuity in the band structure at the half-filled limit depending on whether it is approached from above or below. The jump in the position of the localized d level is of the order of U_d and is shown schematically in Fig. 1.

We end this section with a brief discussion of the way in which strong Coulomb interactions affect the local copper and oxygen compressibilities (called $dn_{\text{Cu}}/d\mu$ and $dn_{\text{O}}/d\mu$, respectively) and the relative occupation factors. We find that $dn_{\text{Cu}}/d\mu$ is small, whereas $dn_{\text{O}}/d\mu$ is of order unity. This effect is common to both the electron and hole pictures, providing there is a metal-insulator transition in the latter. Furthermore, $dn_{\text{Cu}}/d\mu \approx e_0^2 \lambda_0$ so that the copper compressibility vanishes as the insulator is approached. These results which are discussed in more detail in Sec. III indicate that the copper valence is pinned close to Cu^{2+} . Thus, this pinning of the valence is consistent with a Fermi-liquid theory in which there are incipient localization effects.

B. The effects of direct oxygen-oxygen hopping processes: The Fermi surface

In this section we discuss the details of the band structure for two-dimensional copper-oxide systems. For simplicity, we consider only the in-plane bands so that the chain contributions which would be present in $\text{YBa}_2\text{Cu}_3\text{O}_7$ are omitted. The prototype we are considering is, thus, La_2CuO_4 doped with x atoms of strontium per copper atom.

Local-density-functional approximation (LDA) calculations have been carried out on the body-centered tetragonal phase of La_2CuO_4 by several investigators.^{1,2} Near the Fermi energy, E_F , the copper $3d_{x^2-y^2}$ and oxygen $2p_x$ and $2p_y$ bands have strong antibonding character. It has been suggested that the essential features of the band structure near the Fermi energy can be understood in terms of a two-dimensional nearest-neighbor tight-binding model. This approximation is inadequate for the present purposes because it leads to a square Fermi surface at the half-filled limit ($x=0$) and, as will be discussed below, to the wrong sign of the Hall coefficient when excess holes are introduced. LDA-based band-structure calculations^{1,36} find that the Fermi surface becomes more nested as excess holes are introduced by doping with a divalent element. The calculations of Xu *et al.*³⁶ reveal a van Hove singularity in the density of states at a Sr doping concentration of approximately $x=0.17$. In order to simulate these features, it appears that next-nearest-neighbor interactions which come primarily from the hybridization between oxygen $2p_x$ and $2p_y$ orbitals at different sites must be included. The direct Cu-Cu hybridization processes are relatively less important because of the large spatial separation between Cu orbitals.

We include the oxygen-oxygen overlap integrals by adding to the CuO_2 Hamiltonian in Sec. II A, an additional hopping term,

$$\sum_{j,l,\sigma} T_{j,l} (C_{j,\sigma}^\dagger C_{l,\sigma} + C_{l,\sigma}^\dagger C_{j,\sigma}). \quad (2.6)$$

For definiteness in the following, we focus on the electron picture of Sec. II A in which only the valence states Cu^{2+} and Cu^{3+} are present. The mean-field (MF) Hamiltonian with the constraint condition properly incorporated is written as

$$H^{\text{MF}} = \sum_{k,\sigma} \Psi_{k,\sigma}^\dagger M \Psi_{k,\sigma} + \lambda_0 (e_0^2 - 1), \quad (2.7a)$$

where

$$\Psi_{k,\sigma} = \begin{pmatrix} C_{k,\sigma}^x \\ C_{k,\sigma}^y \\ D_{k,\sigma} \end{pmatrix}, \quad M = \begin{pmatrix} \varepsilon_p & T_{xy} & e_0 V_x \\ T_{yx} & \varepsilon_p & e_0 V_y \\ e_0 V_x & e_0 V_y & \varepsilon_d \end{pmatrix}. \quad (2.7b)$$

$$V_x = 2V \cos\left(\frac{k_x a}{2}\right), \quad V_y = 2V \cos\left(\frac{k_y a}{2}\right), \quad (2.7c)$$

$$T_{xy} = T_{yx} = 2T \left[\cos\left(\frac{k_x a}{2} + \frac{k_y a}{2}\right) + \cos\left(\frac{k_x a}{2} - \frac{k_y a}{2}\right) \right], \quad (2.7d)$$

in the auxiliary boson language. By diagonalizing the matrix M , we obtain the renormalized band structure which depends on the variables e_0 and λ_0 . These two parameters are then determined from the two variational equations which are the natural generalization of those obtained for the simpler band structure of the previous section.

It is useful to compare the Fermi surfaces obtained in the present model with those found in full LDA (Refs. 1 and 36) based band-structure calculations. These comparisons are shown in Fig. 2 for three different concentrations of holes labeled (a)–(c) (increasing from left to right). The results of Ref. 36 are shown by the top three panels. In the present model which is shown by the lower sequence of figures, the oxygen-oxygen overlap T is 1 eV and the copper-oxygen hybridization V is 1.6 eV. For the purposes of illustration, these values were chosen to “fit” the band structure results at the largest value of $x=0.2$ where Coulombic renormalizations are least significant. In the lower panel the dashed lines correspond to the Fermi surfaces calculated in the absence of oxygen-oxygen overlap integrals. A comparison with the solid lines thus shows the effects of oxygen-oxygen hopping processes on the Fermi surface shape. A clearly apparent effect of these additional hopping terms is to change the curvature of the Fermi surface from electronlike to holelike. Panel (a) which corresponds to zero or very low concentration of holes ($x \approx 0$) shows that perfect nesting is no longer present when oxygen-oxygen overlap processes are included. Indeed nesting actually becomes stronger for an intermediate concentration of holes which is shown by panel (b). Here $x \sim 0.15$. These observations are reflected in the wave vector dependent susceptibility calculations of Ref. 36. At this intermediate concentration van Hove singularities appear due to the intersection of the Fermi surface with the Brillouin zone. Finally in panel (c), a higher hole concentration of $x \approx 0.2$ is shown to lead to a reduced positive curvature. Ultimately at sufficiently large x the curvature changes sign.

It should be stressed that while the emphasis in this sec-

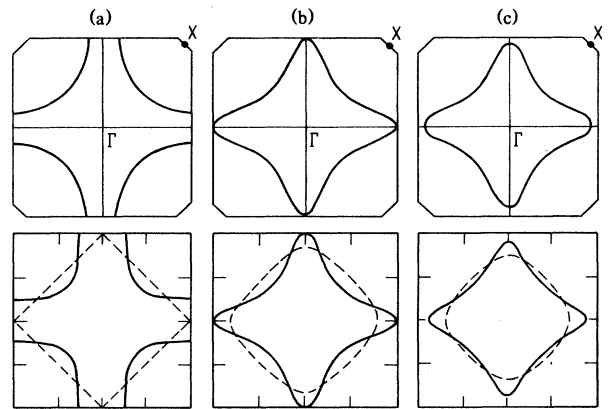


FIG. 2. Comparison of the Fermi-surface shapes as electron filling is varied. Results at top derived from band-structure calculations (Ref. 36); the bottom figures represent the results of the present calculation with (solid) and without (dashed) oxygen-oxygen overlap integrals. Varying from left to right the three hole concentrations are $x \approx 0$, $x \approx 0.15$, and $x \approx 0.2$.

tion has been on demonstrating the necessity for including oxygen-oxygen overlap integrals to model the Fermi surface, there are important effects from Coulomb correlations. As a result of the associated reduction in the copper-oxygen hybridization [see Eq. (2.4)] near the metal-insulator transition, oxygen-oxygen hopping processes become relatively more important. This leads to important changes in the shape of the Fermi surface as seen by a progressively enhanced positive curvature as x approaches 0. This is not present to the same degree in the band-structure results, as can be seen from Fig. 2 by comparing the variations with x within the upper and lower panels.

C. Theory of the Hall coefficient

Hall coefficient measurements on the copper-oxide superconductors have received considerable attention primarily because recent interpretations suggest that they provide evidence for the failure of Fermi-liquid theory. We emphasize these measurements here not only for their relevance to Fermi-liquid theory, but also because they yield information about the general character of the Fermi surface.

$$R_H = - \frac{V_0}{\hbar e} \frac{\int dE \rho(E) v_x [v_x (\partial v_y / \partial k_y) - v_y (\partial v_x / \partial k_x)] \delta[E_i(\mathbf{k}) - E_F]}{\int dE \rho(E) v_x^2 \delta[E_i(\mathbf{k}) - E_F] \int dE \rho(E) v_y^2 \delta[E_i(\mathbf{k}) - E_F]}, \quad (2.8)$$

where $\rho(E)$ is the two-dimensional density of states given by

$$\rho(E) = \int \frac{dl_E}{(2\pi)^2} \frac{1}{|\nabla_{\mathbf{k}} E(\mathbf{k})|}, \quad (2.9)$$

where i is the band index, v_α is the group velocity component of the quasiparticles given by $v_\alpha = (1/\hbar)(\partial E_i / \partial k_\alpha)$. The integration in Eq. (2.9) is done as a line integral along a constant energy line. The quantity $\rho(E)$ depends on the normal velocity and the length of the Fermi line, which in turn depends on the geometry of the Fermi surface. The numerator in Eq. (2.8) is a measure of the average Fermi-surface curvature. This equation is based on the assumption that the quasiparticle lifetimes are sufficiently long and independent of \mathbf{k} . This assumption is expected to fail near the metal-insulator transition. In the context of the present $1/N$ theory, Eq. (2.8) will also be valid when the next order (beyond the mean field) corrections are included only if the real part of the self-energy is independent of \mathbf{k} . If electron-phonon interactions rather than electron-electron interactions are the primary source of the transport lifetime, then it must similarly be assumed that the associated self energy is only weakly \mathbf{k} dependent. Clearly to go beyond the Boltzmann approximation of Eq. (2.8) it will be necessary to develop a more extended transport theory of the copper oxides which also addresses the behavior of the resistivity. While the present calculations assume, for simplicity, that the temperature is zero, it should be noted that experiments reveal a temperature dependence to the Hall coefficient in

As stressed in Ref. 46, in complex band structures, the Hall coefficient does not simply measure the carrier density. A proper calculation of the Hall coefficient must involve Fermi surface integrals of various components of the electron velocities which in turn depend on the details of the band structure. However, using the LDA-based band structure to calculate the Hall coefficient, Allen and co-workers⁴⁶ have not been able to explain the dramatic x dependence which is observed as the insulator is approached. This is not totally unexpected since these LDA calculations do not properly incorporate the metal-insulator transition. Even away from the metal-insulator transition, it appears that the magnitude of the calculated Hall coefficient is significantly less than that measured in most experiments,⁴⁷⁻⁵⁰ although the sign is found to be correct. This suggests that there may be effects associated with "incipient localization" even in the metallic regime.

We may use the linearized Boltzmann transport equation to compute the Hall coefficient. It should be noted that the effects of strong Coulomb correlations do not lead to any modifications in the resultant expression for R_H , as has been discussed in detail by Fukuyama and his collaborators.⁵⁵ The Hall coefficient (at zero temperature) can be expressed as

several copper-oxide-based materials. It is possible that this is a consequence of quasiparticle lifetime effects⁵⁶ although other mechanisms such as structural distortions⁵⁷ may also be important. This temperature dependence will not be discussed here.

Equations (2.8) and (2.9) can be evaluated readily using the renormalized band structure discussed in Sec. II A. In the absence of oxygen-oxygen hopping processes, the quasiparticle velocity components are relatively simple and given by

$$v_\alpha = \frac{1}{\hbar} \frac{e_0^2}{E^+(\mathbf{k}) - E^-(\mathbf{k})} \frac{\partial \gamma_k^2}{\partial k_\alpha}, \quad (2.10)$$

where γ_k is defined below Eq. (2.2). This equation may be readily substituted into Eqs. (2.8) and (2.9) and R_H evaluated numerically. We note at this point that when oxygen-oxygen overlap is neglected R_H vanishes identically at half filling and is negative for $x > 0$. Furthermore, there is essentially a complete cancellation of many-body renormalization effects. These conclusions are radically altered in the presence of oxygen-oxygen hopping processes, as will be discussed in Sec. III.

Incipient localization effects are extremely important in R_H because it involves vanishingly small Fermi-surface velocities in the numerator as well as the denominator. As a consequence, R_H approaches 0/0. In our two-dimensional calculations there is no singular behavior in the Hall coefficient as the insulator is approached. This arises from a cancellation between the divergence in the Fermi-energy density of states and the effects arising from

the vanishing of the velocities. If this divergence is cut off by, for example, a finite dispersion in the direction perpendicular to the planes, then the Hall coefficient will become singular as $x \rightarrow 0$. In reality, the copper oxides are not strictly two-dimensional systems. LDA band-structure calculations¹ find a very weak, but nonvanishing dispersion in the direction perpendicular to the copper-oxide planes (called the z direction). The dominant contribution to this dispersion is probably from oxygen-oxygen hopping processes perpendicular to the planes as well as from a finite d_{z^2} character in the planar copper-oxide bands.⁵⁸ This line of reasoning suggests that near the metal-insulator transition, because of the strong renormalization (reduction) in the copper-oxide hybridization, the z -direction dispersion becomes progressively more important, just as do the oxygen-oxygen hopping processes. The intraplanar insulating behavior thus becomes more comparable to the interplanar conduction. It seems reasonable that these effects may be reflected in the Hall coefficient.

To model the effects of three dimensionality, near to half filling we may write a simple expression for the density of states at the Fermi energy in terms of a three-dimensional dispersion $E(k_x, k_y, k_z)$:

$$\rho(E_F) \approx \int \frac{dS_{E_F}}{(2\pi)^3} \left[\frac{\partial E(\mathbf{k})}{\partial k_z} \right]^{-1}, \text{ as } x \rightarrow 0, \quad (2.11)$$

where the integration is over the constant energy surface and we have assumed that the small velocity in the z direction dominates that in the x and y directions, near the insulating limit ($e_0 \rightarrow 0$). In this limit the Hall coefficient reduces to

$$R_H \approx -\frac{V_0}{e} \frac{1}{e_0^2 \rho(E_F)} K(E_F), \text{ as } e_0^2 \rightarrow 0, \quad x \rightarrow 0, \quad (2.12)$$

where $K(E_F)$ is the measure of the average curvature at the Fermi surface. As the half-filled limit is approached, R_H becomes arbitrarily large since e_0 approaches zero. Note that it follows from Eq. (2.12) that the x dependence of R_H is rather complicated, since e_0 vanishes faster than linearly with x , as will be shown below.

III. NUMERICAL RESULTS

In this section we discuss the results of numerical solution of the mean-field equations and their physical implications for a variety of experiments. We use the band-structure model of Sec. IIB which includes both direct oxygen-oxygen hopping processes as well as copper-oxygen hybridization. For notational simplicity we define the two dimensionless parameters

$$\alpha = V/(\epsilon_p - \epsilon_d^0),$$

$$\beta = T/V,$$

where V is the nearest-neighbor copper-oxygen hopping integral of Eq. (2.7c) and T is the oxygen-oxygen overlap matrix element of Eq. (2.7d). The parameter α measures

the overlap of the copper and oxygen orbitals. In general one should consider both signs of α corresponding to $\epsilon_p > \epsilon_d^0$ and $\epsilon_p < \epsilon_d^0$. There is a strong sentiment in the literature that the *hole* energies are comparable. Therefore, for large U_d , it follows that the *electronic* levels satisfy $\epsilon_p > \epsilon_d^0$. For the sake of generality, we have investigated the effects of $\epsilon_d^0 > \epsilon_p$ and find that the results qualitatively correspond to those of the limit $\epsilon_d^0 < \epsilon_p$, if one considers significantly smaller values of $|\alpha|$ in the first case when comparing to the second. Because of this similarity we will focus only on the case $\epsilon_d^0 < \epsilon_p$ in our numerical calculations.

For lack of more detailed information, we determine the size of α and β from previous band-structure calculations. In the *hole* representation, it has been estimated²³ that $\tilde{\epsilon}_p - \tilde{\epsilon}_d^0$ is around 1 to 2 eV. For definiteness, we take the Coulomb correlation to be 6 eV and the hole level splitting to be $\tilde{\epsilon}_p - \tilde{\epsilon}_d^0 = 2.0$ eV. The former has been determined from XPS spectra^{40,59} to range from about 5 to 7 eV. It then follows that the bare electron d level lies 4 eV below the oxygen level. In the half-filled limit, one can use Hartree-Fock theory to estimate that the splitting between the Hartree-Fock renormalized d level and the oxygen level is then 1 eV. This is consistent with band-structure approaches which find these two energies are nearly degenerate. Realistic values of the hybridization range between 1 and 2 eV.^{1,23} If the hybridization is chosen to be 1.6 eV then the calculated value of α is 0.4. We will use this value for α in most of our numerical calculations. Estimates of β are also in the literature. In Ref. 23 it is argued that β is around 0.5. We have found that within our simplified two parameter band structure these values of β are somewhat large. If we attempt to fit the Fermi-surface shape through the position of the van Hove singularities, found in Ref. 36, then the appropriate value of β lies between 0.125 and 0.25. Most of our calculations assume β to be in this range.

It is important to stress that the band-structure estimates of the covalency parameter α pose problems for both the electron and hole pictures. In the former, it follows that the electron level splitting is $\frac{2}{3}$ the size of the Coulomb energy, which is clearly not in the infinite U_d limit. For the hole picture, $\alpha^{\text{hole}} = 0.8$ which is too large to admit a Brinkman-Rice metal-insulator transition. This serves to emphasize the points made in the Introduction and to indicate that most probably, neither the electron nor the hole pictures are adequate. Rather U_d should be taken to be finite, so that all three valence states are admixed and the distinction between the two pictures does not exist.

In Fig. 3 the density of states $\rho(E)$ is plotted as a function of energy for the antibonding subband. Here we have chosen $\alpha = 0.4$ and $\beta = 0.125$. This density of states is shown for two values of the hole concentration $x = 0.06$ and 0.16 corresponding to the dashed and solid lines, respectively. The units here are arbitrary, since only the ratios of the various energy parameters are specified. The actual values of $\rho(E_F)$ will be discussed later. This figure illustrates in more detail the band narrowing effect which was shown in Fig. 1 (central panel) as the system approaches half filling. On this finer energy scale the van

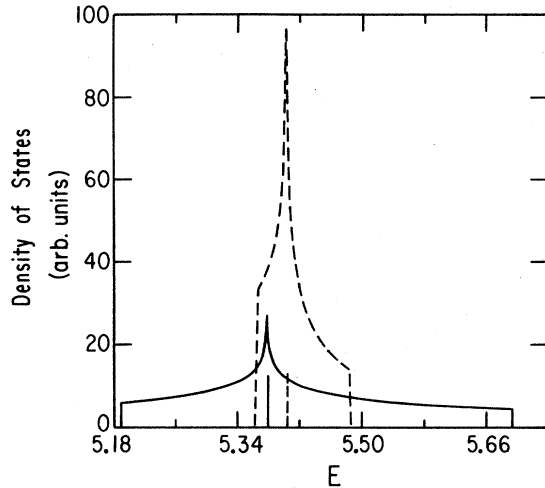


FIG. 3. Energy dependence of the density of states for two values of the hole concentration $x \approx 0.06$ (dashed) and $x \approx 0.16$ (solid). The associated Fermi energies are indicated by the vertical lines.

Hove singularity is clearly apparent. The role of these singularities has been discussed in Ref. 36 and it follows therefore that they are properties of the "one electron" or nonrenormalized energy spectrum and are not affected by strong Coulomb correlations. The role of oxygen-oxygen hopping processes ($\beta \neq 0$) is to introduce an asymmetry in the density of states about the van Hove singularity. Whereas the role of strong Coulomb correlations is to change both the bandwidth as well as its center of gravity.

Considerable attention has been paid to the question of how excess holes are distributed among the copper and oxygen constituents when, say, La_2CuO_4 is doped with Sr.^{4,11} In Figure 4(a) we plot the number of electrons of copper and oxygen character (upper and lower figures) as a function of the total electron count n^{tot} in the electron picture. The half-filled point corresponds to 5 electrons. In order to treat values of n^{tot} above and below five, two different mean-field theoretic sets of equations were solved. The curves were plotted using $\alpha = 0.4$ and for various values of the oxygen-oxygen overlap integrals, given by $\beta = 0.125$ (circles), and $\beta = 0.25$ (triangles). The solid line corresponds to $\beta = 0$. In the absence of oxygen-oxygen hopping processes the excess holes ($n^{\text{tot}} < 5$) are relatively evenly shared among copper and oxygen. The excess electrons ($n^{\text{tot}} > 5$) are entirely taken up by the copper levels since the oxygen bands are essentially fully occupied.

It is important to stress that as the oxygen-oxygen overlap integrals become more appreciable, and when $n^{\text{tot}} < 5$, the copper occupancy rapidly approaches unity. In this way the excess holes reside primarily on the oxygen sites. To understand this, we note that the main obstacle to the localization of the copper levels is the kinetic energy cost. In the absence of oxygen-oxygen hopping ($\beta = 0$) this is prohibitive, so that the holes are rather equally shared among the two types of orbitals, as discussed above. However, as β increases the effects of copper localization are not so costly since there are now other contributions to the

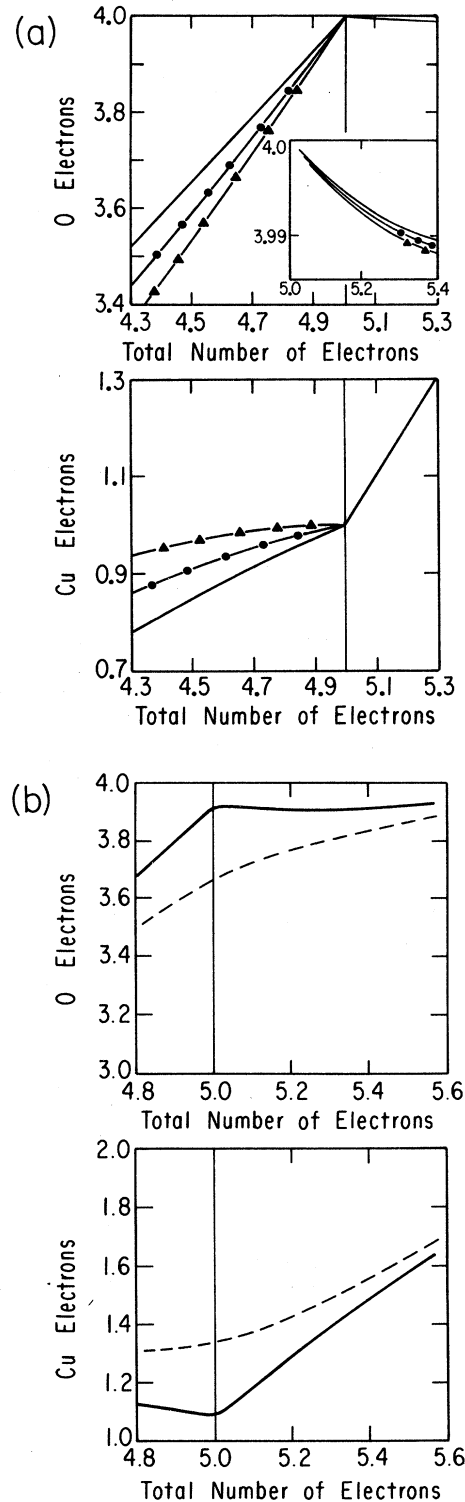


FIG. 4. The partial electron number associated with oxygen and copper components as a function of the total number of electrons. (a) corresponds to the electron model and (b) to the hole model. In the former (a) are shown three values of the oxygen-oxygen overlap integral $\beta = 0$ (solid lines), 0.125 (circles), and 0.25 (triangles). The inset is a blow up of the results above half filling ($n^{\text{tot}} > 5$). In the latter (b) are shown two values of the covalency parameter $\alpha = 0.23$ and 0.35.

kinetic energy. Near half filling the Cu electron count may then be pinned close to unity as shown in Fig. 4(a).

Indeed, it has been generally accepted^{11,60} that in the copper-oxide superconductors the excess holes are associated with the oxygen constituents and Cu is in the Cu^{2+} valence state. We conclude that this is an appropriate picture if there is a moderately strong oxygen-oxygen overlap. This is not then a direct consequence of *only* strong Coulomb interactions, as has been speculated. Furthermore, this “pinning” of the copper valence does not mean that the excess holes are *localized* on any particular oxygen atom, at least not in the metallic regime, considered here. Rather the holes are shared among all oxygen sites. As shown above, it is the very mobility of the oxygen electrons which enables the holes to be preferentially associated with the oxygen atoms.

The behavior of the Fermi liquid when excess electrons are present is quite different. When the band is more than half filled, the copper electron count rises rapidly to accommodate the extra electrons. If U_d is strictly infinite, then the copper filling approaches the limit of 2.0 linearly and the oxygen count is pinned at 4.0. This is because the cost of transferring electrons from the oxygen band to the copper level is prohibitive. For the case of moderately large U_d , there may be some holes in oxygen due to a gain in kinetic energy associated with the oxygen atoms. Thus, the larger the oxygen-oxygen overlap the greater the charge transfer. This very small effect is shown in the inset of Fig. 4(a), where U_d was taken to be 16 eV for the purposes of illustration.

The hole picture [Fig. 4(b)] of Refs. 6 and 7 can be directly compared with the electron picture of Fig. 4(a). In Fig. 4(b) are plotted the number of electrons of copper and oxygen character as a function of n^{tot} . For simplicity we have omitted the oxygen-oxygen overlap integrals. The solid and dashed curves correspond to values of $\alpha^{\text{hole}} = V/(\tilde{\epsilon}_p - \tilde{\epsilon}_d^0)$ which are given by 0.23 and 0.35, respectively. The former case is close to but not yet in the small α^{hole} limit considered in Ref. 6. As can be seen at half filling there is no localization of the Cu electrons since the electron count is always above 1.0. However, for values of α less than 0.2, a localization or metal insulator transition will occur. The smaller value of α in the figure illustrates this trend. For slightly more realistic values of α shown by the dashed line, it is clear that copper is in a mixed valence state so that there is an appreciable fraction of Cu^{1+} present at and around half filling. It is also clear that in this scheme there is a strong tendency for excess holes to be associated with oxygen sites. This is more pronounced than in the case of Fig. 4(a), since here the copper levels contain more than one electron. As a result additional holes are present on the oxygen sites even at half filling. It should be emphasized that in the hole picture the fact that excess holes reside preferentially on the oxygen sites is not equivalent to the statement that the Cu valence is pinned at Cu^{2+} . As can be seen from Fig. 4(b) (dashed line), the copper occupation is pinned close to 1.3 as x varies from 0 to 0.15. This deviation from 1.0 is significantly greater than in the localization picture of Fig. 4(a) in which the copper occupation differs from unity by no more than 5% over this range of concentrations for

both nonzero values of oxygen-oxygen overlap.

A crucial distinction between the two renormalized band models of Figs. 4(a) and 4(b) is seen in the concentration dependence of the effective mass or density of states at the Fermi energy $\rho(E_F)$. In the model of Ref. 7, $\rho(E_F)$ increases with increasing x , or strontium doping. This arises because as x increases the antibonding band narrows (as shown in Fig. 1, left-hand panel), due to the depletion of the Cu^{1+} state relative to the Cu^{2+} state. In this way the copper electrons are more and more localized as holes are added. This is in contrast to what is observed in a model in which there is a localization transition as $x \rightarrow 0$. In this second case [corresponding to Fig. 4(a)], $\rho(E_F)$ increases rapidly as $x \rightarrow 0$. This behavior is illustrated in Fig. 5 for the electron picture. Similar results are obtained in the ionic limit of the hole picture.⁶ Here the density of states at the Fermi energy is plotted as a function of hole concentration x for $\alpha = 0.4$. To obtain the units on the vertical axis we have had to specify the actual copper-oxygen hybridization V (rather than the dimensionless ratio α) in units of eV. For definiteness we chose $V = 1.6$ eV. The two curves correspond to two values of $\beta = 0.25$ (upper curve) and 0.125 (lower curve). We have chosen these two values because they seem to bracket the value which would best fit the Fermi-surface shape. We estimate that $\beta \approx 0.18$ may be most appropriate. However, to show the effects of varying oxygen-oxygen overlap integrals we have presented our results with two somewhat extreme limits of β .

There are some experimental indications of the size and x dependence of $\rho(E_F)$ which do not seem to be consistent with this localization picture, although the data is quite uncertain at this time. It has been estimated that Sommerfeld constants obtained in $\text{La}_{2-x}\text{Sr}_x\text{CuO}_4$ range^{61,62} between about 6 and 12 mJ/molK² at $x = 0.15$. This translates to $\rho(E_F)$ between 2.5 and 5 states/eVcell. At higher concentrations, $x = 0.2$, the reported values^{63,64} of γ range between about 14 and 39 mJ/molK² correspond-

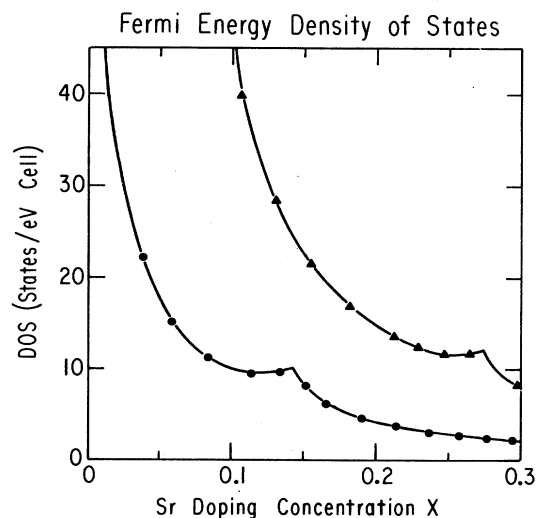


FIG. 5. Density of states at the Fermi energy as a function of hole concentration x for the same parameters as in Fig. 4(a).

ing to a $\rho(E_F)$ of 6 to 17 states/eV cell. These measured values of $\rho(E_F)$ are considerably lower than shown in the figure. For a lower limit, we estimate $\rho(E_F)=10$ states/eV cell at $x\sim 0.15$. In the localization picture the copper-oxide superconductors would behave like “moderately heavy” fermions. Furthermore, the x dependence does not seem to be correct. However, it should be noted that for $x\sim 0.2$ there are problems in $\text{La}_{2-x}\text{Sr}_x\text{CuO}_4$ with controlling the oxygen stoichiometry.⁶⁵ To help establish the x dependence of $\rho(E_F)$ it would be better to look in a lower range of x values, say between 0.08 and 0.17, where oxygen stoichiometry is well controlled. It should also be stressed that extracting the values of γ are difficult experiments which must be done on high quality samples. Specific heat and magnetic susceptibility χ measurements are not likely to yield unambiguous results, because the former is dominated by the lattice contribution in the normal state¹⁵ and there are temperature dependences in the latter whose origin is not entirely certain.¹⁶⁻²⁰ It should also be noted that in narrow band metals there may be additional temperature dependences in χ coming from the electronic contribution as has been discussed in Ref. 30. If the insulator is driven by a localization transition, then it seems clear that $\rho(E_F)$ or γ must increase as x decreases near $x\approx 0$. However, it is not possible to quantitatively predict the magnitude of γ since (i) three-dimensional effects may tend to cut off the singularity and (ii) a more accurate band structure must be used. We should also note that in the metallic regime we find that other competing effects such as van Hove singularities may mask the structure reflecting the localization transition.

It is noteworthy that while there is little evidence for a dramatic x dependence in the Sommerfeld constant as the insulator is approached, the Hall coefficient is extremely sensitive to changes in x near $x=0$. In Fig. 6(a), by way of a summary, we have replotted a variety of different Hall coefficient measurements⁴⁷⁻⁵⁰ as a function of strontium concentration in doped La_2CuO_4 . While there is considerable scatter in the data (some of which reflects the temperature dependence of R_H) one trend is clear: R_H rapidly increases as $x\rightarrow 0$. It should be stressed, however, that interpreting experiments on polycrystalline samples is somewhat complex as has been emphasized in Ref. 66.

To try to understand this behavior we have calculated the x dependence of R_H using the same parameters as in Fig. 5. The results are shown in Fig. 6(b). The circles correspond to $\beta=0.125$ and the triangles to $\beta=0.25$, obtained using Eq. (2.8) in a strictly two-dimensional model. The small kinks which are evident on both curves are a reflection of the geometry of the Fermi surface. The curvature of the Fermi surface increases monotonically with decreasing x , whereas the length of the Fermi line is maximum near the van Hove singularities. This leads to the structure shown in the figure. Similar effects were also seen in the density of states calculation of Fig. 5. To represent the experimental situation, we have replotted the data of Ref. 49 shown by the solid squares. The curves *A* and *B* are from previous calculations. The latter corresponds to the LDA based calculations⁴⁶ and the former is

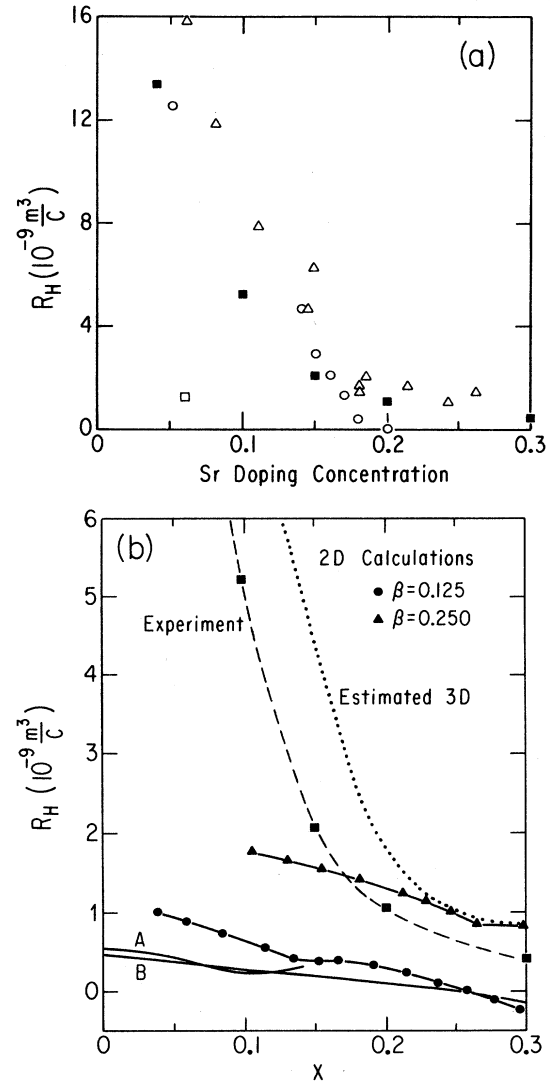


FIG. 6. (a) Experimentally measured Hall coefficient as a function of strontium doping in La_2CuO_4 from Ref. 48 (triangles), Ref. 47 (circles), and Ref. 49 (squares). The open square indicates one single-crystal measurement from Ref. 49. (b) Comparison of different theoretical results for Hall coefficient as a function of hole concentration. The curves labeled *A* and *B* are from Refs. 7 and 46, respectively. The present results are shown for the same parameters as in Fig. 4(a) by the circles and triangles (2D calculations) and by the dotted line (estimated 3D results) for the larger value of β . We have selected the data of Ref. 49 to plot for comparison purposes (squares).

taken from Ref. 7 in which the renormalized band-structure approach with infinite hole-hole repulsion was used. These previous theoretical results are not in good agreement with most experiments as may be seen from the figure. A comparison of the two curves *A* and *B* shows that they are rather similar so that the effects of infinite Coulomb correlations are not clearly apparent in R_H within the hole-hole repulsion picture of Ref. 7. (The small upturn around $x\approx 0.1$ is, presumably, a manifesta-

tion of the decreasing renormalized bandwidth discussed earlier). The localization model leads to a larger Hall coefficient particularly as $x \rightarrow 0$. This is a reflection of the increased importance of oxygen-oxygen hopping relative to the copper-oxygen hybridization terms as the insulator is approached. These oxygen-oxygen processes contribute to a positive Hall coefficient so that the greater their relative weight, the larger the (positive) Hall coefficient. Indirectly then, in our calculations the growth in R_H as $x \rightarrow 0$ derives from incipient localization processes. For $\beta \approx 0.18$, which seems to match the Fermi-surface shape, we anticipate that the present two-dimensional model would yield reasonable agreement with the measured R_H for $x \geq 0.15$. However, it is clear that in a strictly two-dimensional model R_H will never increase sufficiently rapidly as $x \rightarrow 0$, to be consistent with experiment.

As discussed in Sec. IIC, the effects of three dimensionality on the Hall coefficient are rather profound, since a three-dimensional dispersion may cut off the singularity in the density of states $\rho(E_F)$ as $x \rightarrow 0$ and thus, as shown in Eq. (2.12) lead to a greatly enhanced Hall coefficient. It is extremely difficult to obtain a reliable estimate of these three-dimensional (3D) effects because of the difficulties inherent in calculating a 3D Fermi surface in the presence of strong Coulomb correlations. Presumably one should introduce additional oxygen bands (corresponding to overlap processes in the z direction). This would involve diagonalizing a 7×7 matrix in conjunction with solving the mean-field equations. As a rough estimate we have included a Cu d_{z^2} along with an oxygen p_z band which thus reduces to a 5×5 problem. Rather than solving self-consistently for the mean-field equations in this larger matrix we have replaced the 3×3 submatrix by that arising in our 2D mean-field theory in the absence of any z -direction coupling. Phenomenological overlap integrals V_z associated with the z direction are chosen so that away from half filling the ratio of the z bandwidth to xy bandwidth is $\frac{1}{100}$. Furthermore, the strong constraint of Luttinger's theorem is imposed so that the Fermi volume in the 3D model with no dispersion in the z direction is the same as that of 3D model with the Fermi volume derived from the above scheme.

In Fig. 7 is shown the resulting 3D Fermi surface for an irreducible wedge. Figures 7(a)–7(c) correspond to vary-

ing hole concentrations of $x = 0.04, 0.13,$ and 0.21 , respectively. Our choices of $\alpha = 0.4$ and $\beta = 0.125$ correspond to parameters used throughout this section. The effective z -direction hopping matrix element is $V_z/V = 0.06$. The solid lines indicate the irreducible wedge of our simplified model and the dashed lines correspond to that of the LDA where a more complex lattice structure is considered. The shaded area indicates the occupied Fermi volume. There are clear similarities between the results of our simple model and the LDA calculated Fermi surface in the metallic region as can be seen by comparing Figs. 7(b) and 7(c) with Figs. 1(b) and 1(c) in Ref. 36. However as shown in Fig. 7(a) incipient localization effects very near the metal-insulator transition lead to important differences between the LDA and the present theory. The dotted lines plot our 3D Fermi surface as extrapolated towards $x \rightarrow 0$. (It should be understood that our Fermi-liquid approach is not valid arbitrarily close to $x = 0$, but our intention here is to emphasize the trends with varying small x).

Even with the approximations for the Fermi surface discussed above, it is still difficult to evaluate R_H numerically. To estimate the Hall coefficient, we perform the indicated Fermi-surface integrals by using a coarse mesh in which the 2D contributions to R_H from slices perpendicular to the z direction are summed with equal weight. The behavior of each Hall coefficient contribution is described by Eqs. (2.9) and (2.10). With reference to the dotted lines in Fig. 7(a), although the flat region of the Fermi surface is larger, because of the short Fermi line length, the region of positive curvature dominates the Hall coefficient. Consequently, R_H rises rapidly as $x \rightarrow 0$. A semiquantitative estimate for R_H is shown by the dotted line in the figure for the case of $\beta = 0.25$. Presumably this case represents an overestimate of the oxygen-oxygen hopping processes so that in the metallic regime, the Cu electrons are more strongly localized than would be expected. Thus, these 3D effects begin to show up at a relatively high hole concentration $x \approx 0.15$. For the smaller value of $\beta \approx 0.125$, the 3D enhancement of R_H coming from incipient localization will occur at significantly smaller x values. A more realistic case would lie between the two limits. Although fully self-consistent mean-field calculations are required, these crude estimates illustrate the fact

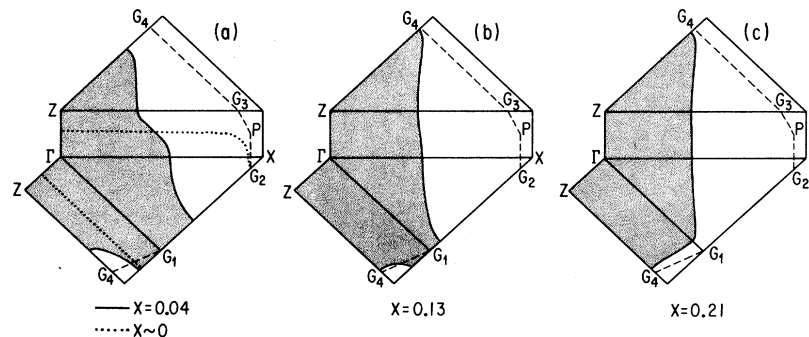


FIG. 7. Evolution of the 3D Fermi surface with varying hole concentration (a) $x = 0.04$, (b) $x = 0.13$, and (c) $x = 0.21$. The dashed lines correspond to the LDA calculated irreducible wedge which differs from that of the present simplified model. The zone of the present model is indicated by the outermost solid lines. The dotted lines in (a) correspond to the limiting $x \approx 0$ Fermi-surface shape.

that incipient localization effects may lead to a diverging Hall coefficient as x approaches zero, providing some small three-dimensional dispersion is included.

IV. CONCLUSIONS

The main contribution of this paper has been to describe a Fermi liquid in which both a semirealistic band structure of the copper and oxygen components and incipient localization phenomena are included. We have emphasized that the interplay between these two effects is important for understanding the copper oxides. It should be stressed that there have been previous attempts to incorporate one or the other of these two phenomena into a Fermi-liquid scheme,^{6,7} but not both. Thus, this represents a kind of "collaboration" between band-structure approaches and strong Coulomb correlation theories which give rise to localization. It also represents an intermediate picture between those theories in which the copper is fully localized and the band picture in which it is covalently admixed with the oxygen. We do not believe that this general picture is limited by $1/N$ expansion approaches or infinite U_d theories. One should view this more generally as a plausible scenario for a Fermi-liquid theory of the copper oxides.

To what extent is this scenario valid? We have argued that it is consistent with the observation that the copper valence is pinned close to Cu^{2+} and with the general behavior of the Hall coefficient. However, the most stringent test of this picture is based on the behavior of the Sommerfeld coefficient γ as the metal-insulator transition is approached. This coefficient should grow rapidly as the transition is reached. This behavior should be apparent, although to a lesser degree, even within the metallic or Fermi-liquid regime, just as the Hall coefficient seems to reflect the onset of localization. On the basis of thermodynamic measurements, there is as yet no indication of this incipient localization in γ when either x is varied in $\text{La}_{2-x}\text{Sr}_x\text{CuO}_4$ or as oxygen stoichiometry is varied in $\text{YBa}_2\text{Cu}_3\text{O}_7$. These are difficult experiments which require well characterized samples, particularly since, as discussed in the Introduction, γ cannot be obtained yet in a simple direct way either from specific heat¹⁵ or static susceptibility¹⁶⁻²⁰ measurements. One may speculate that thermodynamic measurements are not as direct a probe of the localization transition (if it exists) as are transport measurements, such as the ac and dc conductivities and the Hall coefficient. These latter measurements have a number of features which seem consistent with an effective mass which increases as the insulator is approached. On the other hand, all of these transport measurements may also be interpreted in terms of a Hubbard gap or reduced carrier number description. The ultimately decisive experiments may well be Fermi-surface studies.

In this paper we have not addressed the interactions in the Fermi liquid. Within the $1/N$ scheme these can be readily calculated.^{6,25-27} These interactions occur as a result of fluctuations of the renormalized copper-oxygen hybridization as well as fluctuations of the copper d level. In the limit of infinite U_d and to leading order in $1/N$, these

interactions do not involve a spin-spin coupling which might be important in these materials. Nevertheless, we can make some general comments and speculations about the magnetism and superconductivity associated with the Fermi liquid.

Because this theory leads to a localization of the Cu electrons at half filling, the natural description of the magnetism in the insulating state is that of a Heisenberg local spin model in which the interactions derive from superexchange. In the electron picture, there is no superexchange mechanism at infinite U_d , whereas for the hole picture⁶ a charge transfer contribution $J = 4V^4/(\tilde{\epsilon}_p - \tilde{\epsilon}_d^0)^3$ is present. That these two pictures lead to different results is a consequence of infinite U_d . As was seen earlier, in the hole picture there is considerably more delocalization so that charge transfer exchange can take place. These two approaches become equivalent at finite U_d which seems to be more appropriate for the copper oxides. Presumably there is a "residue" of this superexchange in the metallic state, which can in principle be incorporated into a Fermi-liquid approach. However, it should be stressed that even without these interaction induced spin fluctuation effects there will be considerable structure in the dynamical susceptibility $\chi_0(\mathbf{q}, \omega)$, deriving from the interplay of band structure and localization effects. Analogous effects have been discussed in the context of heavy fermions.⁶⁷ Calculations of this dynamical susceptibility are in progress and should provide a basis for extracting from experiment the residual spin fluctuation effects.

At this stage it seems premature to focus on the superconducting mechanism, since the picture of the normal state is still uncertain. It is, nevertheless, amusing to speculate about different pairing interactions. For the most part, treatments of the superconductivity are based on a description of the metallic state in terms of a disordered Heisenberg antiferromagnet in the presence of dilute, mobile holes. These treatments have yielded novel and exotic scenarios for the superconductivity involving quasiparticles of various statistics: Fermi,¹⁰ Bose,⁶⁸ and fractional.⁶⁹ Experimental proof for the existence of these quasiparticles is still very controversial. In a somewhat different vein, Newns and co-workers⁷ have argued that a finite U_d mean-field theory of the copper oxides (which we have discussed here for infinite U_d) may lead to superconductivity. In this approach both the Cu^{1+} and Cu^{3+} bosons are assumed to co-exist at the same site. If one chooses to replace both bosons with c numbers, the resulting mean-field theory breaks global gauge invariance and number conservation and, therefore, has been associated with superconductivity. This approach is still controversial⁷⁰ and its interpretation requires that the effects of finite U_d on the normal state must also be sorted out.

More generally, it is evident that the nature of the normal state is far from clear at this point. Knowing the extent to which the copper electrons are localized will help select among a variety of different scenarios (e.g., the band picture, incipient localization of Cu in a Fermi liquid, and full localized Cu spins) of these systems.

In summary, it is our contention that if a Fermi-liquid description is appropriate, the large body of evidence which implies that the Cu valence is pinned close to $+2$

suggests that this Fermi liquid is nearly localized. This behavior is reminiscent of helium-3 and f electrons in heavy electron metals. Localization strongly affects the Hall coefficient since it involves the ratio of nearly vanishing conductivities. While the localization mechanism we have considered is Brinkman-Rice (Coulomb) localization, the general behavior we have found for the Hall coefficient and other properties would also be obtained if incipient localization derived from other effects.

Note added in proof. Our calculations on excess electron systems are, in principle, relevant to the newly discovered electron doped oxides [Y. Tokura, H. Takagi, and S. Uchida, *Nature* (London) **337**, 345 (1989)]. However, it should be noted that the observed change in the sign of R_H in these materials is not compatible with the LDA calculated Fermi-surface shape which is only slightly modified from that in the hole-doped systems.

ACKNOWLEDGMENTS

We thank M. Suzuki for providing us with his data prior to publication. Useful conversations with J. J. Yu, R. Martin, A. J. Freeman, J. Burdett, and P. A. Allen are acknowledged. This work was supported by National Science Foundation Grant No. DMR 84-20187, National Science Foundation—Materials Research Laboratory Grant No. DMR-16892, and U.S. Department of Energy Grant No. DE-AC02-76H00016. K. L. acknowledges the hospitality and many stimulating conversations with numerous colleagues (most notably, E. Alp, B. Dunlap, G. Crabtree, and D. Koehling) at Argonne National Laboratory. This paper was presented as a thesis by J.H.K. to the Department of Physics, The University of Chicago, in partial fulfillment of the requirements for the Ph.D. degree.

*Present address: Physics Department, Boston University, Boston, MA 02215.

¹J. M. Tranquada, S. M. Heald, and A. R. Moodenbaugh, *Phys. Rev. B* **36**, 5263 (1987); J. M. Tranquada, S. M. Heald, A. R. Moodenbaugh, and M. Suenaga, *Phys. Rev. B* **35**, 7187 (1987).

²E. D. Crozier, N. Alberding, K. R. Bauchspiess, A. J. Seary, and S. Gyax, *Phys. Rev. B* **36**, 8288 (1987); J. A. Yarmoff, D. R. Clarke, W. Drube, H. O. Karlsson, A. T. Ibrahim, and F. J. Himpsel, *Phys. Rev. B* **36**, 3967 (1987).

³L. F. Mattheiss, *Phys. Rev. Lett.* **58**, 1028 (1987); J. Yu, A. J. Freeman, and J. H. Xu, *Phys. Rev. Lett.* **58**, 1035 (1987).

⁴W. E. Pickett, H. Krakauer, D. A. Papaconstantopoulos, and L. L. Boyer, *Phys. Rev. B* **35**, 7253 (1987).

⁵T. C. Leung, X. W. Wang, and B. N. Harmon, *Phys. Rev. B* **37**, 384 (1988).

⁶G. Kotliar, P. A. Lee, and N. Read, *Physica C* **153-155**, 538 (1988).

⁷D. M. Newns, P. Pattnaik, M. Rasolt, and D. A. Papaconstantopoulos, *Phys. Rev. B* **38**, 7033 (1988); D. M. Newns, M. Rasolt, and P. Pattnaik, *ibid.* **38**, 6513 (1988).

⁸G. Kotliar and A. Ruckenstein, *Phys. Rev. Lett.* **57**, 1362 (1986).

⁹C. M. Varma, S. Schmitt-Rink, and E. Abrahams, *Phys. Rev. Lett.* **26**, 2793 (1988); V. J. Emery, *Phys. Rev. Lett.* **58**, 2794 (1984).

¹⁰P. W. Anderson, *Science* **235**, 1196 (1987); P. W. Anderson, G. Baskaran, Z. Zou, and T. Hsu, *Phys. Rev. Lett.* **58**, 2790 (1987).

¹¹D. C. Johnston, J. P. Stokes, D. P. Goshorn, and J. T. Lewandowski, *Phys. Rev. B* **36**, 4007 (1987); Y. Endoh, K. Yamada, R. J. Birgeneau, D. R. Gabbe, H. P. Janssen, M. A. Kastner, C. J. Peters, P. J. Picone, T. R. Thurston, J. M. Tranquada, G. Shirane, Y. Hidaka, M. Oda, Y. Enomoto, M. Suzuki, and T. Murakami, *Phys. Rev. B* **37**, 7443 (1988).

¹²J. M. Luttinger, *Phys. Rev.* **119**, 1153 (1960).

¹³L. C. Smedskjaer, J. Z. Liu, R. Benedek, D. G. Legnini, D. J. Lam, M. D. Stahulak, H. Claus, and A. Bansil, *Physica C* **156**, 296 (1988); A. Bansil, R. Pakaluoto, R. S. Rao, P. Mijnaerends, W. Dlugosz, R. Prasad, and L. Smedskjaer, *Phys. Rev. Lett.* **61**, 2480 (1988).

¹⁴(a) M. Lee, J. Thiel, W. P. Halperin, S. J. Hwu, and K. R. Poppelmeier, *Phys. Rev. B* **36**, 2378 (1987). It is somewhat

puzzling that nuclear quadrupole resonance (NQR) relaxation at the planar sites in the 1:2:3 compounds does not exhibit a Korringa behavior in contrast to NMR in the 2:1:4 material. See, for example, P. C. Hammel, M. Takigawa, R. H. Heffer, and Z. Fisk, *Phys. Rev. B* **38**, 2832 (1988). This may, in part, be due to additional charge fluctuation mechanisms for NQR relaxation. (b) R. S. List, A. J. Arko, Z. Fisk, S.-W. Cheong, S. D. Conradson, J. D. Thompson, C. B. Pierce, D. E. Peterson, R. J. Bartlett, N. D. Shinn, J. E. Schirber, B. W. Veal, A. P. Paulikas, and J. C. Campuzano, *Phys. Rev. B* **38**, 11966 (1988).

¹⁵R. A. Fisher, J. E. Gordon, and N. E. Phillips, *J. Supercond.* (to be published).

¹⁶R. L. Greene, H. Maletta, T. S. Plaskett, J. G. Bednorz, and K. A. Müller, *Solid State Commun.* **63**, 379 (1987); H. Takagi, S. Uchida, H. Sato, K. Kitazawa, K. Fueki, and S. Tanaka, *Jpn. J. Appl. Phys.* **26**, Suppl. 26-3, 1029 (1987).

¹⁷D. C. Johnston, S. K. Sinha, A. J. Jacobson, and J. Newson, *Physica C* **153-155**, 572 (1988).

¹⁸S. W. Cheong, S. E. Brown, Z. Fisk, R. S. Kwok, J. D. Thompson, E. Zirngiebl, G. Gruner, D. E. Peterson, G. L. Wells, R. B. Schwarz, and J. R. Cooper, *Phys. Rev. B* **36**, 3913 (1987); J. M. Tarascon, L. H. Greene, B. G. Bagley, and W. R. McKinnon, in *Novel Superconductivity*, edited by S. A. Wolf and V. Z. Kresnin (Plenum, New York, 1987).

¹⁹B. Barbara, A. F. Khoder, M. Couach, A. Ayache, E. Bonjour, and R. Calemczuk, *Physica C* **153-155**, 912 (1988).

²⁰A. Bezinge, A. Junod, T. Graf, J. Muller, M. Francois, and K. Yvon, *Physica C* **153-155**, 1513 (1988).

²¹G. R. Stewart, *Rev. Mod. Phys.* **56**, 775 (1984).

²²L. Taillefer, R. Newbury, G. G. Lonzarich, Z. Fisk, and J. L. Smith, *J. Magn. Magn. Mater.* **63-64**, 372 (1987).

²³See, for example, A. K. McMahan, R. M. Martin, and S. Satpathy, *Phys. Rev. B* **38**, 6650 (1988).

²⁴For a review of heavy fermion theories, see, for example, P. A. Lee, T. M. Rice, J. W. Serene, L. J. Sham, and J. W. Wilkins, *Comments Solid State Phys.* **12**, 98 (1986).

²⁵A. Auerbach and K. Levin, *Phys. Rev. Lett.* **57**, 877 (1986).

²⁶A. J. Millis and P. A. Lee, *Phys. Rev. B* **35**, 3394 (1987).

²⁷T. M. Rice and K. Ueda, *Phys. Rev. Lett.* **55**, 995 (1985).

²⁸B. H. Brandow, *Phys. Rev. B* **33**, 215 (1986).

²⁹J. Zaanen, O. Jepsen, O. Gunnarsson, A. T. Paxton, O. K. Andersen, and A. Svane, *Physica C* **153-155**, 1637 (1988).

- ³⁰*The Metallic and Nonmetallic State of Matter*, edited by P. P. Edwards and C. N. R. Rao (Taylor and Francis, London, 1985).
- ³¹G. A. Sawatzky and J. W. Allen, *Phys. Rev. Lett.* **53**, 2339 (1984); J. Zaanen, G. A. Sawatzky, and J. W. Allen, *Phys. Rev. Lett.* **55**, 418 (1985).
- ³²See, for example, T. V. Ramakrishnan in Ref. 30.
- ³³J. Hubbard, *Proc. R. Soc. London Ser. A* **276**, 238 (1963).
- ³⁴W. F. Brinkman and T. M. Rice, *Phys. Rev. B* **2**, 4302 (1970).
- ³⁵D. A. Huse and V. Elser, *Phys. Rev. Lett.* **60**, 2531 (1988).
- ³⁶J. H. Xu, T. J. Watson-Yang, J. Yu, and A. J. Freeman, *Phys. Lett. A* **120**, 489 (1987).
- ³⁷D. P. Arovas and A. Auerbach, *Phys. Rev. B* **38**, 316 (1988).
- ³⁸A. Auerbach and D. P. Arovas, *Phys. Rev. Lett.* **61**, 617 (1988).
- ³⁹For a recent brief review of some of these issues see H. Rietschel, J. Fink, E. Gering, F. Gompf, N. Nucker, L. Pintschovius, B. Renker, W. Reichardt, H. Schmidt, and W. Weber, *Physica C* **153–155**, 1067 (1988), and references therein.
- ⁴⁰Z. Shen, J. W. Allen, J. J. Yeh, J. S. Kang, W. Ellis, W. Spicer, I. Lindau, M. B. Maple, Y. D. Dalichaouch, M. S. Torikavili, J. Z. Sun, and T. H. Geballe, *Phys. Rev. B* **36**, 8414 (1987).
- ⁴¹E. E. Alp (private communication); W. Herzog, M. Schwarz, H. Sixl, and R. Hoppe, *Z. Phys. B* **71**, 19 (1988); T. Takahashi, F. Maeda, H. Katayama-Yoshida, Y. Okabe, T. Suzuki, A. Fujimori, S. Hosoya, S. Shamoto, and M. Sato, *Phys. Rev. B* **37**, 9788 (1988).
- ⁴²P. Steiner, S. Hufner, V. Kinsinger, I. Sander, B. Siegwart, H. Schmitt, R. Schulz, S. Junk, G. Schwitzgebel, A. Gold, C. Politis, H. P. Muller, R. Hoppe, S. Kemmler-Sack, and C. Kunz, *Z. Phys. B* **69**, 449 (1988); M. Ospelt, J. Henz, E. Kaldis, and P. Wachter, *Physica C* **153–155**, 159 (1988); E. E. Alp, G. K. Shenoy, D. G. Hinks, D. W. Capone, L. Sonderholm, H. Schuttler, J. Guo, D. E. Ellis, P. A. Montano, and M. Ramanathan, *Phys. Rev. B* **35**, 1799 (1987).
- ⁴³H. Oyanagi, H. Ihara, T. Matsushita, M. Tokumoto, M. Hirobayashi, N. Terada, K. Senzaki, Y. Kimura, and T. Yao, *Jpn. J. Appl. Phys.* **26**, L488 (1987); N. Nucker, J. Fink, B. Renker, D. Ewert, P. J. W. Weijs, and J. Fuggle, *Jpn. J. Appl. Phys.* **26**, Suppl. 26-3, 1015 (1987).
- ⁴⁴E. E. Alp, L. Soderholm, G. K. Shenoy, D. G. Hinks, B. W. Veal, and P. Montano, *Physica B* **150**, 74 (1988).
- ⁴⁵D. H. Kim, D. D. Berkley, A. M. Goldman, R. K. Schulze, and M. L. Mecartney, *Phys. Rev. B* **37**, 9745 (1988); B. Lengeler, M. Wilhelm, B. Jobst, W. Schwoen, B. Seebacher, and U. Hillebrecht, *Physica C* **153–155**, 143 (1988).
- ⁴⁶P. B. Allen, W. E. Pickett, and H. Krakauer, *Phys. Rev. B* **36**, 3926 (1987); P. B. Allen, W. E. Pickett, and H. Krakauer, *Phys. Rev. B* **37**, 7482 (1988).
- ⁴⁷N. P. Ong, Z. Z. Wang, J. Clayhold, J. M. Tarascon, L. H. Greene, and W. R. Mckinnon, *Phys. Rev. B* **35**, 8807 (1987).
- ⁴⁸M. W. Shafer, T. Penney, and B. L. Olson, *Phys. Rev. B* **36**, 4047 (1987).
- ⁴⁹M. Suzuki, *Phys. Rev. B* **39**, 2312 (1989); see also M. Suzuki and T. Murakami, *Jpn. J. Appl. Phys.* **26**, 524 (1987).
- ⁵⁰S. W. Tozer, A. W. Kleinsasser, T. Penny, D. Kaiser, and F. Holtzberg, *Phys. Rev. Lett.* **59**, 1768 (1987).
- ⁵¹M. Gurevitch and A. T. Fiory, *Phys. Rev. Lett.* **59**, 1337 (1987).
- ⁵²S. Barnes, *J. Phys. F* **6**, 1375 (1976); **7**, 2632 (1977); P. Coleman, *Phys. Rev. B* **35**, 5072 (1987).
- ⁵³A. Auerbach and K. Levin, *Phys. Rev. B* **34**, 3524 (1986).
- ⁵⁴N. Read and D. M. Newns, *J. Phys. C* **16**, 3273 (1983); N. Read, *J. Phys. C* **18**, 2651 (1985).
- ⁵⁵For a recent paper on this subject, see, e.g., Y. Hasegawa and H. Fukuyama (unpublished), where the Hall coefficient has been discussed in the context of resonating-valence-bond theory.
- ⁵⁶P. A. Lee and N. Read, *Phys. Rev. Lett.* **58**, 2691 (1987).
- ⁵⁷S. Bhattacharya, M. J. Higgins, D. C. Johnston, A. J. Jacobson, and J. P. Stokes, *Phys. Rev. Lett.* **60**, 1181 (1988).
- ⁵⁸A. J. Freeman, D. Koelling, B. Harmon, and W. E. Pickett (private communications).
- ⁵⁹D. van der Marel, J. van Elp, G. A. Sawatzky, and D. Heitmann, *Phys. Rev. B* **37**, 5136 (1988); A. Fujimori, E. Takayama-Muromachi, Y. Uchida, and B. Okai, *Phys. Rev. B* **35**, 8814 (1987).
- ⁶⁰A. Aharony, R. J. Birgeneau, A. Coniglio, M. A. Kastner, and H. E. Stanley, *Phys. Rev. Lett.* **60**, 1330 (1988).
- ⁶¹W. K. Kwok, G. W. Crabtree, D. G. Hinks, D. W. Capone, J. D. Jorgensen, and Z. Zhang, *Phys. Rev. B* **35**, 5343 (1987); M. V. Nevitt, G. W. Crabtree, and T. E. Klippert, *Phys. Rev. B* **36**, 2398 (1987).
- ⁶²B. Batlogg, A. P. Ramirez, R. J. Cava, R. B. van Dover, and E. A. Rietman, *Phys. Rev. B* **35**, 5340 (1987).
- ⁶³G. Niewa, E. N. Martinez, F. de la Cruz, D. A. Esparza, and C. A. D'Ovidio, *Phys. Rev. B* **36**, 8780 (1987).
- ⁶⁴J. M. Ferreira, B. W. Lee, Y. Dalichaouch, M. S. Torikavilli, K. N. Yang, and M. B. Maple, *Phys. Rev. B* **37**, 1580 (1988); M. E. Reeves, T. A. Friedman, and D. M. Ginsberg, *Phys. Rev. B* **35**, 7207 (1987).
- ⁶⁵J. Jorgensen, *Jpn. J. Appl. Phys.* **26**, Suppl. 26-3, 2017 (1987).
- ⁶⁶D. Stroud and P. M. Hui, *Phys. Rev. B* **37**, 8719 (1987).
- ⁶⁷A. Auerbach, J. H. Kim, L. Levin, and M. R. Norman, *Phys. Rev. Lett.* **60**, 623 (1988).
- ⁶⁸S. A. Kivelson, D. S. Rokhsar, and J. P. Sethna, *Phys. Rev. B* **35**, 8865 (1987).
- ⁶⁹R. B. Laughlin, *Phys. Rev. Lett.* **60**, 2677 (1988).
- ⁷⁰For example, A. Auerbach (unpublished) has shown that such a state cannot be a minimum of the free energy.